JOURNAL OF MATERIALS SCIENCE 24 (1989) 432-438

Effects of firing temperature on morphology and crystal structure of zirconium *bis*(monohydrogen phosphate) and its alkali salts

Y. SADAOKA, M. MATSUGUCHI, Y. SAKAI, S. MITSUI, M. TOITA, K. HATANAKA
Department of Industrial Chemistry, Faculty of Engineering, Ehime University, Matsuyama 790, Japan

In zirconium *bis*(monohydrogen phosphate)monohydrate, the stability of water of crystallization and of the crystal form was strongly influenced by its crystal size. The water of crystallization of a smaller crystal was completely released on heating to 200° C while a part of this water was held at 300° C in a larger crystal with a diameter of several micrometres. While a smaller crystal was decomposed by heating to 900° C and cubic zirconium pyrophosphate was formed, for a larger crystal, α-layered zirconium pyrophosphate was formed instead of cubic zirconium pyrophosphate and a layered structure was held. For the Na_2-, K_2- and Rb_2-forms, good layer structure was retained even by heating to 1000° C. For the Li_2-form, the layer structure was decomposed on heating at or above 900° C. The thermal stability of the layered structure increased with increasing crystal size and ionic radii of the alkali cation.

1. Introduction

It is well known that inorganic electrolytes are formed by polybasic acids and certain hydrolysable polyvalent cations, and many of these salts are extremely insoluble in most reagents; typical examples are the phosphates of zirconium and titanium. Of these, zirconium phosphate is known to be an insoluble inorganic ion exchanger and proton conductor. In zirconium *bis*(monohydrogen phosphate)monohydrate, the structure of which is well known, each layer consists of a plane of zirconium atoms bridged through tetrahedral phosphate groups located alternatively above and below in this plane. While zirconium phosphate is a useful material as a proton conductor, the protonic conductivity is strongly influenced by the degree of hydration and the stability of hydrated water molecules [1–4]. To determine the behaviour of hydrated water and dehydration processes, thermogravimetrical studies for zirconium *bis*(monohydrogen phosphate) have been carried out [5–7] and the weight loss process can be expressed as follows

$$Zr(HPO_4)_2\,H_2O \xrightarrow{150^\circ C} Zr(HPO_4)_2 \quad (1)$$

$$Zr(HPO_4)_2 \xrightarrow{550^\circ C} ZrP_2O_7 \quad (2)$$

but the effects of crystal size on the dehydration were not discussed.

On the other hand, it is expected that zirconium *bis*(monohydrogen phosphate) will be a useful material as a starting reagent to prepare ionic conductive ceramics [8] because the acidic protons are easily exchanged by small ions such as Li^+, Na^+, K^+, etc., and its concentration can be controlled by the regulation of pH in zirconium *bis*(monohydrogen phosphate)-dispersed solution.

This report describes the results of an investigation of the effect of heat-treatment on the morphologies and crystal form of zirconium *bis*(monohydrogen phosphate) and its alkali salts and the effect of crystal size on the dehydration.

2. Experimental details

Three types of zirconium *bis*(monohydrogen phosphate) were prepared: (1) by refluxing amorphous zirconium phosphate with phosphate acid for 100 h (CZP100), (2) by the same refluxing for 400 h (CZP400), (3) by precipitation of zirconium phosphate by adding phosphoric acid to zirconium fluorate solution in a bubbling stream of nitrogen gas (FZP).

The average particle diameters were determined to 0.55, 2.4 and 5.8 μm for CZP100, CZP400 and FZP, respectively. Alkali salt was obtained by titrating FZP suspended in deionized water for Li_2-, Na_2- and K_2-forms and/or deionized water containing a small number of sodium ions for Rb_2- and Cs_2-forms with the corresponding alkali hydroxide solution. All the crystals were washed with distilled and deionized water and dried at 60° C. The powder was pressed into a disc at 200 kg cm^{-2} and fired at each temperature for 2 h. Measurements were made using a standard X-ray diffractometer, thermogravimetry and scanning electron microscopy.

 0022-2461/89 $03.00 + .12

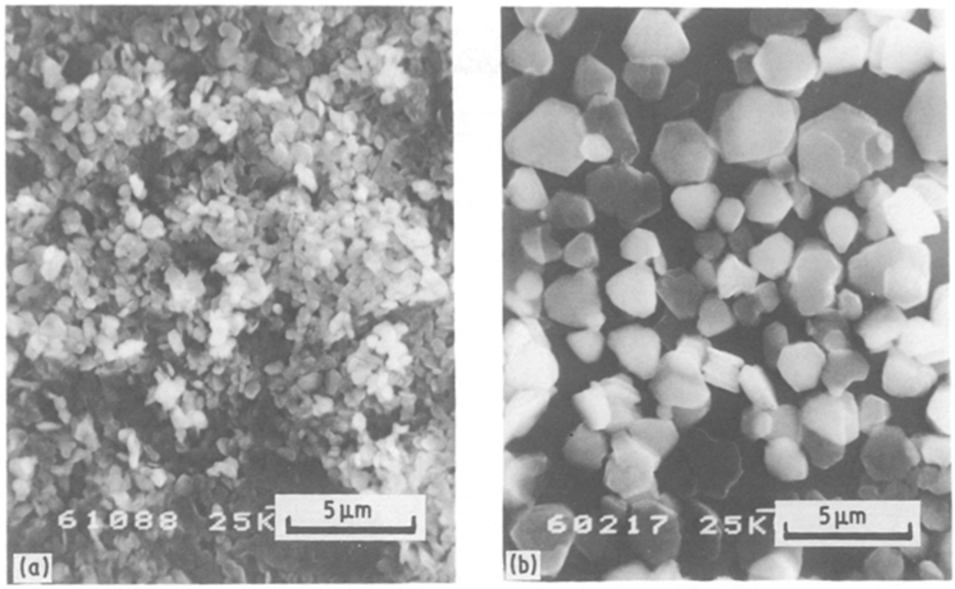

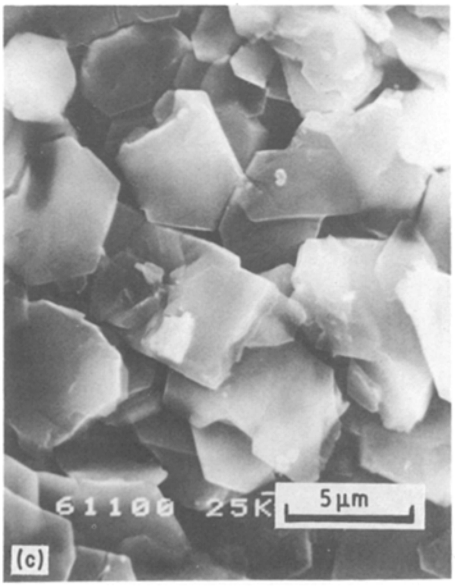

Figure 1 External views of crystals dried at 60° C. (a) CZP100, (b) CZP400, (c) FZP.

3. Results and discussion

3.1. Zirconium *bis*(monohydrogen phosphate)monohydrate

The crystal forms were examined by scanning electron microscopy as shown in Fig. 1. The crystal size falls in the order FZP > CZP400 > CZP100. All the samples have a layered structure and the ratio of the length perpendicular to the layer to that parallel to it, decreases with crystal size. The results of thermal analysis are shown in Fig. 2. For CZP100, the first weight loss was observed in the temperature region from 100° C to 170° C, the second in the region from 200 to 350° C and the third in the region 450 to 600° C. While the characteristic temperatures in the thermal analysis were not affected by the crystal size, the degree of the first weight loss was lowered and the second loss increased with increasing size. The weight loss observed in the temperature region below 400° C corresponded to Process 1, i.e. the dehydration of the water of crystallization, and the third weight loss to the dehydration of hydrogen phosphate (Process 2). These results indicate that the dehydration temperature of the water of crystallization increases and its rate decreases with an increase in crystal size, i.e. the stability of the crystal form depends upon the size. The XRD patterns are summarized in Table I. For a smaller crystal, i.e. CZP100, the *d*-value corresponded to the interlayer distance changing from 0.756 to 0.656 nm; its peak intensity was lowered and its width at half-height increased with increasing firing temperature up to 600° C; in addition, all the observed

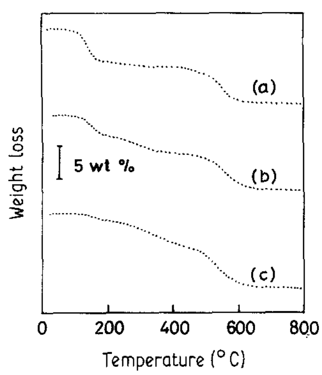

Figure 2 Thermogravimetric analysis curves of crystals. (a) CZP100, (b) CZP400, (c) FZP. Heating rate 5° C min^{-1}.

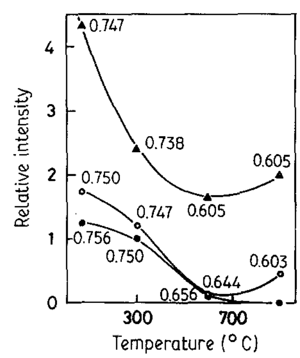

Figure 3 Relationship between relative intensity of diffraction peak and the firing temperature. (●) CZP100, (○) CZP400, (▲) FZP. *d*-values (nm) are indicated in the figure.

TABLE I XRD patterns of CZP100, CZP400 and FZP fired at various temperatures

	60° C		300° C		600° C		900° C	
	d (nm)	I/I_0	d (nm)	I/I_0	d (nm)	I/I_0	d (nm)	I/I_0
CZP100	0.756	63	0.750	100	0.656	67	0.478	33
	0.447	43	0.452	41	0.452	100	0.414	100
	0.355	100	0.360	56			0.369	35
	0.352	56					0.337	32
	0.264	30	0.264	33	0.267	67	0.292	32
	0.262	30					0.249	42
	0.240	13					0.189	12
	0.204	11					0.184	21
CZP400	0.750	100	0.747	100	0.644	86	0.603	44
	0.446	31	0.452	29	0.617	71	0.473	24
	0.355	98	0.359	38	0.448	100	0.410	100
	0.351	55			0.422	86	0.368	29
	0.264	30	0.264	23	0.267	71	0.335	22
	0.262	26					0.291	25
	0.240	17					0.264	9
							0.248	31
FZP	0.747	100	0.738	100	0.605	100	0.605	100
	0.445	12	0.451	8				
	0.354	41	0.355	12	0.415	19	0.414	35
	0.351	23	0.310	11	0.403	12	0.404	20
	0.264	12	0.264	7	0.265	9	0.288	11
	0.261	10	0.261	7			0.264	9
	0.240	8						

d-values were assigned to cubic zirconium pyrophosphate (ZrP_2O_7) for the sample fired at 900° C for a 2 h hold. Clearfield and Stynes [9] reported that the interlayer distance of α-$Zr(HPO_4)_2 \cdot xH_2O$ ($x = 0, 1$) was 0.756 nm and independent of the degree of hydration. But for CZP100 fired at 300° C which was assigned to α-$Zr(HPO_4)_2$, the interlayer distance was estimated to be 0.750 nm and slightly smaller than that reported and similar decrements in the interlayer distance on heating at 300° C were confirmed in the other crystals. On heating to 600° C, the XRD patterns and their relative intensity were varied, i.e. the highest peaks observed at 0.750 nm for CZP100 and 0.747 nm for CZP400 fired at 300° C disappeared, the relative intensity of peaks at 0.452 nm for CZP100 and 0.448 nm for CZP400 increased, and the peak at 0.656 nm for

TABLE II XRD patterns of ion-exchanged FZP

	60° C				1000° C			
	d (nm)	I/I_0	d (nm)	I/I_0	d (nm)	I/I_0	d (nm)	I/I_0
Li_2	0.886	100	0.277	3	0.563	17	0.314	37
	0.441	10	0.262	6	0.442	100	0.310	20
	0.410	11	0.221	5	0.397	18	0.275	21
	0.359	23			0.377	27	0.255	27
	0.321	8			0.336	17		
Na_2	0.993	100	0.385	8	0.769	100	0.339	14
	0.852	8	0.371	8	0.439	17	0.332	14
	0.494	7	0.361	9	0.390	15	0.288	11
	0.446	9	0.352	8	0.380	22	0.265	25
	0.417	23	0.343	19	0.351	23	0.254	16
K_2	0.903	100	0.356	38	0.907	100	0.201	21
	0.463	28	0.304	80	0.403	42		
	0.436	49	0.271	37	0.319	58		
	0.392	70	0.263	43	0.259	17		
	0.367	20			0.249	7		
Rb_2	0.932	45	0.308	24	0.924	51	0.266	28
	0.419	16	0.268	39	0.460	5	0.229	8
	0.409	26	0.231	12	0.413	46	0.223	7
	0.332	100	0.214	13	0.325	100	0.205	35
	0.320	34	0.204	23	0.306	20	0.201	21
Cs_2	0.423	40	0.216	22	0.950	10	0.271	32
	0.337	100			0.473	15	0.236	14
	0.324	58			0.421	44	0.228	10
	0.270	46			0.334	100	0.211	37
	0.242	28			0.315	43	0.205	23

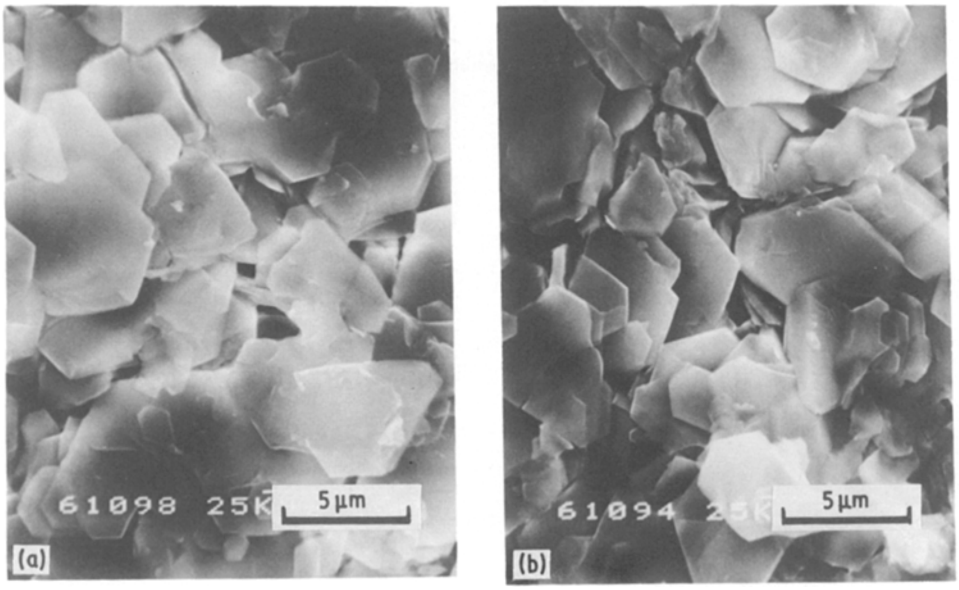

Figure 4 External views of FZP, fired at: (a) 600° C, (b) 1000° C.

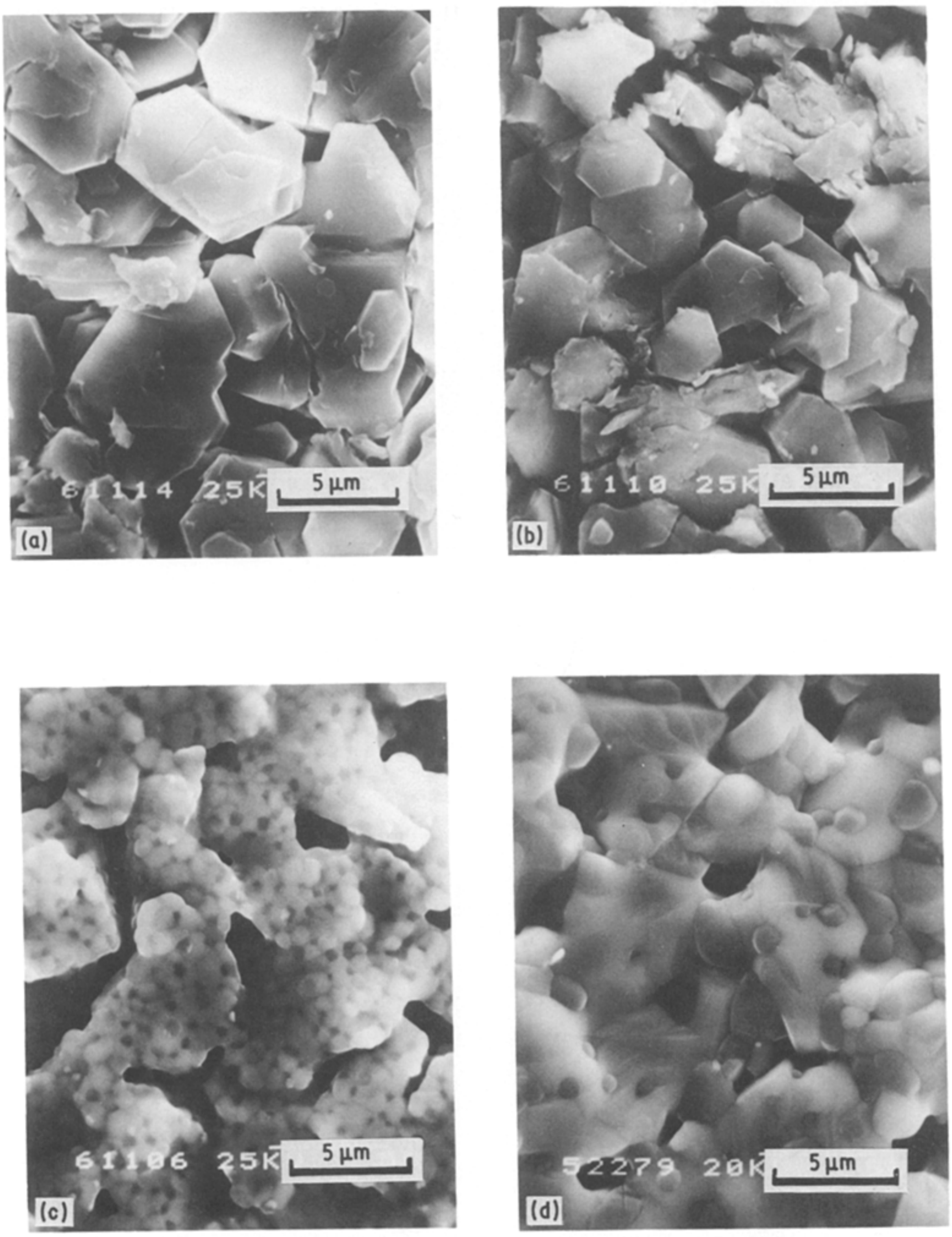

Figure 5 External views of the Li_2-form of FZP. (a) 60° C, (b) 600° C for 2 h, (c) 1000° C for 2 h, (d) 1000° C for 16 h.

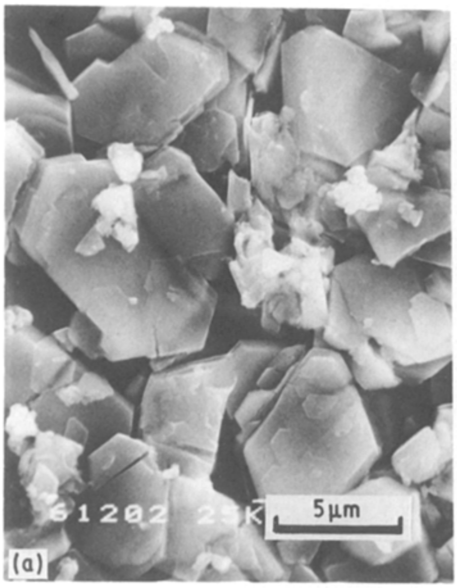

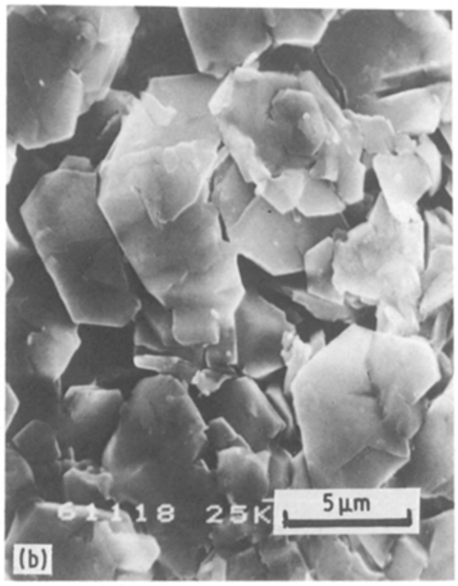

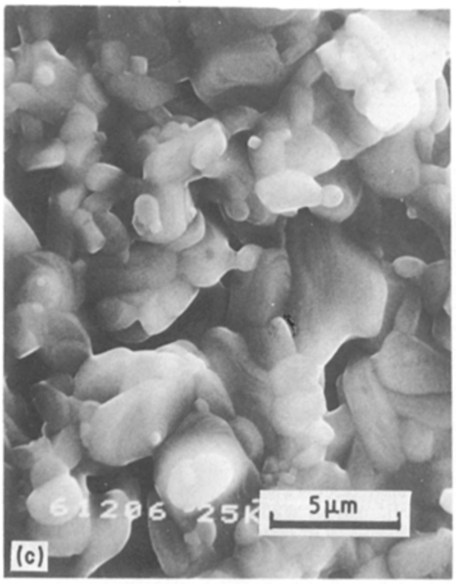

Figure 6 External views of the Na_2-form of FZP. (a) 60° C, (b) 600° C, (c) 1000° C.

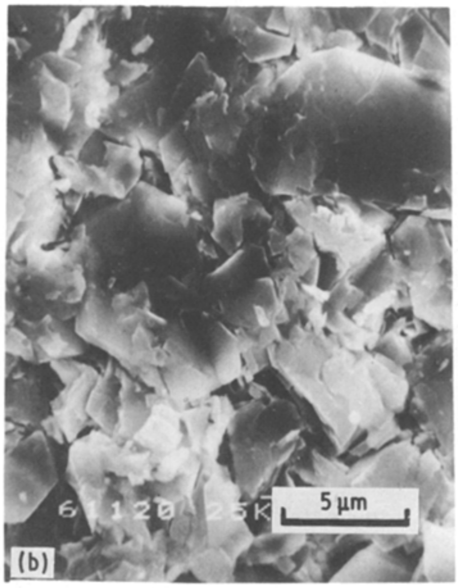

Figure 7 External views of the K_2-form of FZP. (a) 60° C, (b) 600° C, (c) 1000° C.

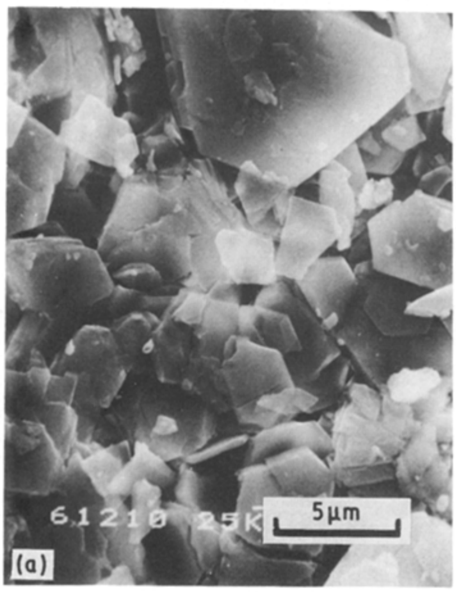

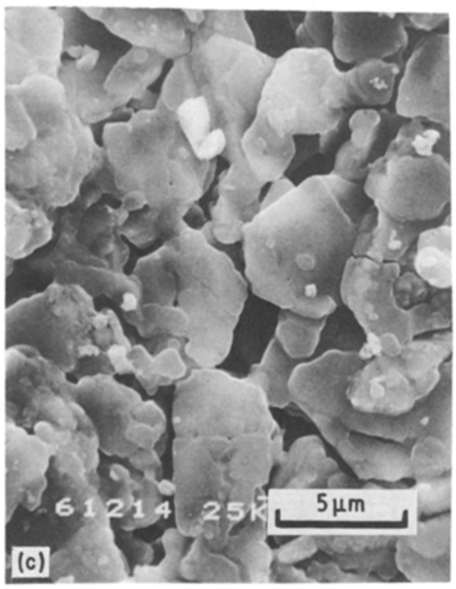

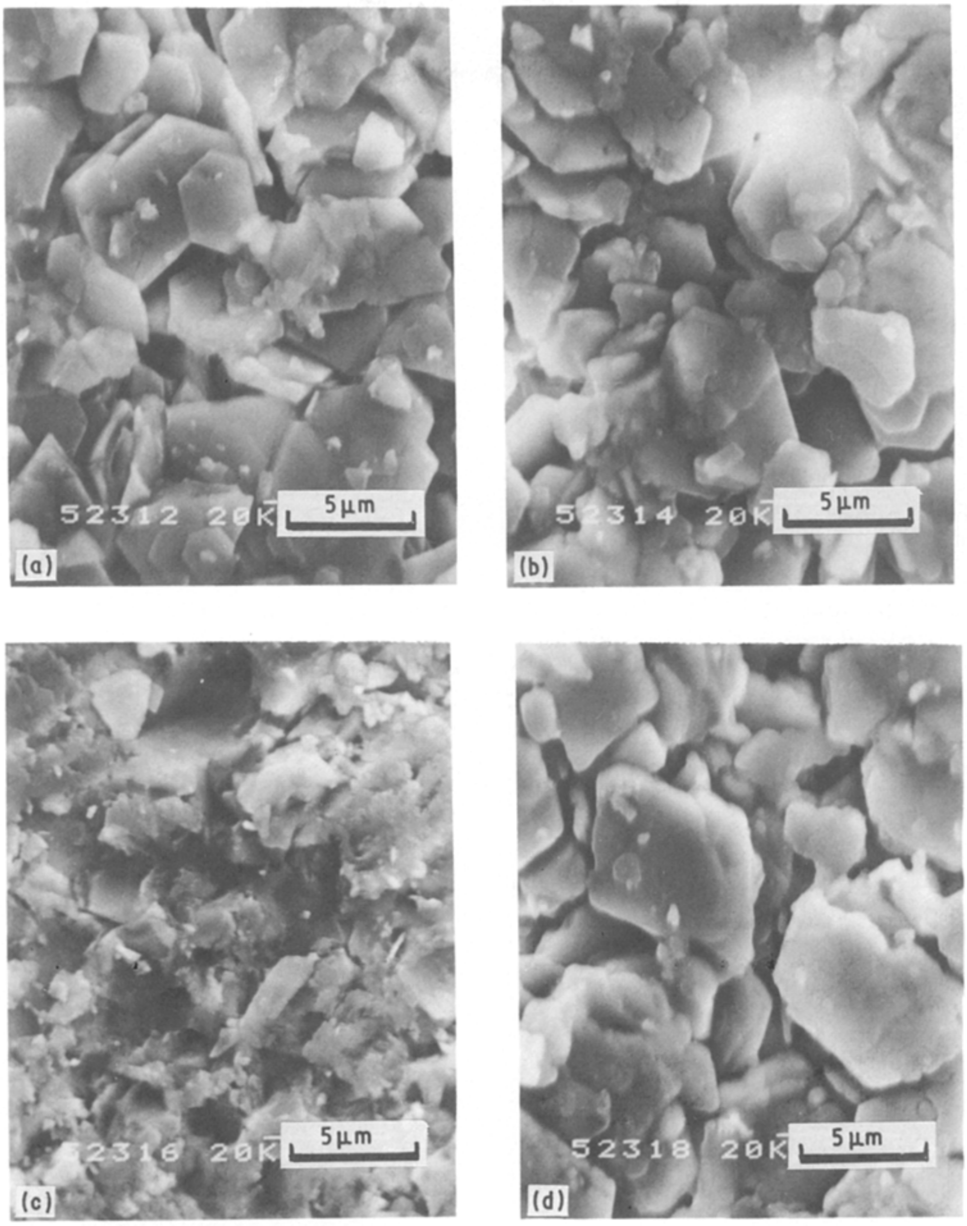

Figure 8 External views of the Rb_2- and Cs_2-forms of FZP. (a) 60° C, (b) 1000° C for Rb_2-form. (c) 60° C, (d) 1000° C for Cs_2-form.

CZP100 and 0.644 nm for CZP400 appeared, while for FZP, the peak at 0.703 nm diminished and a new peak appeared at 0.605 nm. Furthermore, for the sample fired at 900° C, all the peaks observed for CZP100 were assigned to cubic zirconium pyrophosphate as mentioned above, while some peaks which could not be assigned to cubic zirconium pyrophosphate were observed for CZP400 and FZP. For comparison, the relationship between the relative intensity of the peak corresponded to the interlayer distance and the firing temperature, was shown in Fig. 3. The intensity was lowered and then increased for CZP400 and FZP, while the *d*-value decreased monotonically to ~0.60 nm with increasing firing temperature. From these results, it was observed that the dehydration procedure accompanied the deformation of crystals and the stability of the layered structure increased with crystal size. Fig. 4 shows the microstructure of FZP fired at each temperature. Clearly, it was confirmed that the decomposition of a layered structure was not induced by the heat treatments and α-layered zirconium pyrophosphate was formed by the heat treatment for larger crystals.

3.2. Fully ion-exchanged crystals

The thermal analysis and titration indicate that the protons were completely exchanged by Li^+, Na^+ and K^+ and 95% or more of protons by Rb^+ and Cs^+.

The microstructure of the crystals dried at 60° C and fired at 600 and 1000° C is shown in Figs 5 to 8. For the sample dried at 60° C, the external appearance of FZP were little influenced by replacing the protons by alkali cations (Li^+, Na^+, K^+, Rb^+), while the crystallinity of the caesium form was lowered. Similar external appearances were observed for the sample fired at 600° C. By heating at 1000° C for 2 h, the form and microstructure were changed. For the Li_2-form FZP, the layer structures were decomposed and new smaller crystals appeared.

For the Na_2- and K_2-forms, traces of partial melting were confirmed, while it seems that each crystal retains a layered structure. Furthermore, no distinct variation in the external appearance of the Rb_2-form were confirmed and the crystallinity of the Cs_2-form increased. The crystal structures were examined by X-ray diffraction (XRD). The confirmed XRD patterns are summarized in Table II. The peaks corresponded to the interlayer distance which disappeared for the Li_2-form and was confirmed for the other alkali forms fired at 1000° C.

These variations were consistent with the results of observation of the external appearances by SEM. Except for the Li-form, the *d*-values confirmed for the sample fired at 1000° C were consistent with the interlayer distance [10] for anhydrous phases of crystalline zirconium phosphate completely exchanged with monovalent cation and the layer structure was retained even after heating to 1000° C. For the Li_2-form, the XRD results indicate that the new form (phase J) confirmed by Clearfield *et al.* [6] was formed by heating at 900° C for 2 h. While phase J was confirmed for the sample fired at 1000° C for 2 h, prolonged firing for 16 h induced the formation of lithium dizirconium triphosphate and the fusion of the small crystals proceeded as shown in Fig. 5. In addition, sodium dizirconium triphosphate was formed as a minor product for the Na_2-form fired at 1000° C for 2 h, while potassium dizirconium triphosphate was not formed by the same heat-treatment.

References

1. E. KROGH ANDERSEN, I. G. KROGH ANDERSEN, C. KNAKKERGÅRD MØLLER, K. E. SIMONSEN and E. SKOU, *Solid State Ionics* **7** (1982) 301.
2. S. YDE-ANDERSEN, J. S. LUNDSGÅRD, J. MALLING and J. JENSEN, *ibid.* **13** (1984) 81.
3. G. ALBERTI, M. CASCIOLA, U. CONSTANTINO, G. LEVI and G. RICCIARDI, *J. Inorg. Nucl. Chem.* **40** (1978) 533.
4. G. ALBERTI, M. CASCIOLA, U. CONSTANTINO and M. LEONARDI, *Solid State Ionics* **14** (1984) 289.
5. A. DYER, D. LEIGH and F. T. OCON, *J. Inorg. Nucl. Chem.* **33** (1971) 3141.
6. A. CLEARFIELD, S. P. PACK and J. M. TROUP, *ibid.* **39** (1977) 1437.
7. Y. INOUE and Y. YAMADA, *Bull. Chem. Soc. Jpn* **52** (1979) 3528.
8. Y. SADAOKA and Y. SAKAI, *J. Mater. Sci. Lett.* **5** (1986) 731.
9. A. CLEARFIELD and J. A. STYNES, *J. Inorg. Nucl. Chem.* **26** (1964) 117.
10. G. ALBERTI and U. CONSTANTINO, *J. Chromatography* **102** (1974) 5.

Received 22 January
and accepted 10 June 1988